Environmental Coastal Regions

EDITOR:

C.A. Brebbia
Wessex Institute of Technology

WIT PRESS Boston, Southampton
Computational Mechanics Publications

Cyclic movement of water particles in a coastal aquifer

H. Sun[a], M. Koch[b]
[a]*Department of Geological Sciences, Rider University, Lawrenceville, NJ 08648, USA*
[b]*Department of Geohydraulics and Engineering Hydrology, University of Kassel, Kurt-Wolters Straße 3, 34109 Kassel, Germany*

Abstract

The movement of water particles in a coastal aquifer is controlled not only by the regional flow, but also by the rising and falling of the tidal levels in the coastal water. This combined influence results in periodic variations of the hydraulic gradient with ensuing cyclic movements of water particles in a coastal aquifer. Based on a two-dimensional analytical series solution for the piezometric head in response to tidal loading, these cyclic movements are theoretically investigated. The approach is then applied to the New Jersey coastal aquifer near Atlantic City. Amplitudes and phases of 25 tidal constituents are calculated using standard harmonic analysis. After appropriate filtering of the observed piezometric heads, a calibration for the storativity/transmissivity (S/T) ratios is carried out. The latter are found to decrease with increasing hydraulic pressure which appears to be consistent with the idea of a reduced aquifer compressibility with higher pressure. Eventually, water particle trajectories in the aquifer are calculated using Darcy's law. The trajectories of a ground water particle demonstrate a cyclic flow path caused by the tidal wave, creating a unique 'flushing' effect in the coastal aquifer. This 'flushing' phenomenon should be taken into consideration when the transport or removal of a solute or contaminant within a coastal aquifer is modeled.

1 Introduction

Piezometric heads in a coastal aquifer rise during high tide and fall during low tide, causing periodic variations of the hydraulic gradient, with a subsequent change also of the direction and magnitude of the flow. On top of these tidal influences the movement of water particles is driven by the regional flow, with the result that zigzag flow paths arise in a coastal aquifer. This cyclic movement of water particles in a coastal aquifer is similar to the progressive movement of water particles in open water except that it is confined in the pore space of rocks, and therefore its magnitude limited by the hydraulic properties of the aquifer, e.g. transmissivity and storativity.

While there have been a few studies of one-dimensional (1D) piezometric head's response to tidal loading (e.g. *Greg, 1966; Carr and Van Der Kamp, 1969; Hsieh et al.,1989; Nielsen, 1990; Serfes, 1992; Yim and Mohsen, 1992*), no comprehensive investigations of 2D water particle movements have been carried out to-date. This study is an extension of earlier work of *Sun (1997)* on the 2D analytical solution for the groundwater response to tidal loading, but with emphasis on the calibration of the transmissivity/storativity (S/T)-ratio and on the analysis of water particle trajectories in coastal aquifers. The results of this investigation are important for further understanding coastal hydrology and for modeling contaminant transport in a coastal aquifer.

2 Mathematical theory

2.1 Analytical solution for piezometric head's response to tidal loading

The hydraulic head h [L] in a horizontal (x-y domain) confined, nonleaky, homogeneous aquifer is governed by the 2D *groundwater flow equation*

$$\frac{\partial^2 h}{\partial x^2} + \frac{\partial^2 h}{\partial y^2} = \frac{S}{T}\frac{\partial h}{\partial t} \qquad (1)$$

(cf. *Bear, 1972*), where t [T] is the time; S, storativity; T [L^2/T] = kB, transmissivity; k, hydraulic conductivity [L/T]; B [L] aquifer thickness. Eq. (1) is solved in a domain that extends in x-direction from the coast x=0, inland to x =∝, and whose y-axis is aligned along the coast or an estuary.

The initial condition is $h(x,y,t=0)=0$ and the two boundary conditions are (1) the coastal tidal bc.

$$h_{tide}(x,y,t) = H_0 + \sum_{k=1}^{n} A_k e^{-p_k x - m_k y} \cos(\omega_k t - b_k y - q_k x + \varphi_k) \qquad (2)$$

and (2) the far-inland bc. $h(\infty,y,t)=0$. Eq (2) describes a damped tidal wave consisting of a superposition of n tidal constituents traveling along-shore in y-direction into an estuary (*Dean and Dalrymple, 1984*). Notations are: A_k, amplitude; m_k, damping factor; $\omega_k = 2\pi/T_k$, angular tidal velocity; T_k, tidal period; b_k, wavenumber; and φ_k, phase of the kth tidal constituent. ω_k and b_k are related through $b_k \approx \omega_k / c_0$, where c_0 is the shallow-water phase speed.

With the coastal bc. (2), the tidal solution of the groundwater flow eq. (1) can be written as a linear superposition of all tidal constituents

$$h_{tide}(x,y,t) = H_0 + \sum_{k=1}^{n} A_k e^{-p_k x - m_k y} \cos(\omega_k t - b_k y - q_k x + \varphi_k) \qquad (3)$$

Insertion of this expression into eq. (2) results in terms for (*Sun, 1997*)

$$p_k = \left[\sqrt{(b_k^2 - m_k^2)^2 + (\omega_k S/T - 2b_k m_k)^2} + b_k^2 - m_k^2\right]^{1/2} / \sqrt{2} \qquad (4)$$

and

$$q_k = (\omega_k S/T - 2b_k m_k) / 2p_k \,. \qquad (5)$$

With regional flow included, using the superposition principle (*Bear, 1972*), the total 2-D potentiometric head in a coastal aquifer is then written as

$$h(x,y,t) = h_{reg}(x,y,t) + h_{tide}(x,y,t) \qquad (6)$$

2.1 Calculation of water particle trajectories

Assuming a constant regional hydraulic gradient $\nabla h_{reg} = (f_x, f_y)^T$, the application of Darcy's law $\mathbf{v} = -k\nabla h$ to eq. (6), together with eq. (3), results in the following expression for the x-component $u(t)$ of the flow velocity $\mathbf{v}$

$$\begin{aligned} u = -kf_x &+ k\sum_{k=1}^{n} A_k p_k e^{-p_k x - m_k y}\cos(\omega_k t - b_k y - q_k x + \varphi_k) \\ &- k\sum_{k=1}^{n} A_k q_k e^{-p_k x - m_k y}\sin(\omega_k t - b_k y - q_k x + \varphi_k) \end{aligned} \qquad (7)$$

and a corresponding one for the y-component $v(t)$. Knowing these local velocities u and v at a particular location (x_0, y_0) and time t_o, the x_1-coordinate of the new position (x_1, y_1) of the particle at time t_1 can be computed through

$$x_1 = x_o + \int_{t_o}^{t_1} u(t)\,dt$$

$$= x_o - kf_x t \Big|_{t_o}^{t_1} + k\sum_{k=1}^{n}\left(\frac{A_k p_k}{\omega_k} e^{-p_k x - m_k y} \sin(\omega_k t - b_k y - q_k x + \varphi_k) \Big|_{t_o}^{t_1} \right)$$
$$+ k\sum_{k=1}^{n}\left(\frac{A_k q_k}{\omega_k} e^{-p_k x - m_k y} \cos(\omega_k t - b_k y - q_k x + \varphi_k) \Big|_{t_o}^{t_1} \right) \quad (8)$$

and a corresponding one for the the y_1-coordinate. Repeated application of eq. (8) between times t_n and t_{n+1} ($n=1,..,nmax$) provides the loci of the trajectory of a water particle in the aquifer between x_1 and x_{nmax}.

3 Application to the New Jersey coastal aquifer

The above theory is applied to a section of the New Jersey coastal aquifer near Atlantic City, NJ. Hourly piezometric head data from the USGS monitor wells *Galen*, 590m inland from the coastline, and *Firehouse*, 350m inland (*Fig. 1*)---that both tap the confined 800-foot sand of the Kirkwood Formation--- were obtained for July 1994 (*USGS, 1994*), together with tidal levels (NOAA). The analysis of this data in accordance with the theory of Section 2 is carried out in three steps.

3.1 Harmonic tidal analysis

Tidal amplitudes and phases of up to 25 total tidal constituents for the use of eq. (2) are calculated from the NOAA tidal data series by means of a standard harmonic analysis (*Boon and Kiley, 1978*) Results for the six major components are shown in *Table 1*. The wavenumber b_k is calculated from $b_k = \omega_k / c_0$, where c_0, the phase speed is given by $c_0 = (gd)^{1/2}$, with d the average water depth (=2m for the NJ coastal section in the study area), and g, the gravity acceleration.

Table 1: *Results for the first six components of the tidal series expansion*

No	*Tide*	*Velocity* ω_k *[degree/h]*	*Amplitude* A_k *[cm]*	*Phase* φ_k *[degree]*
1	M2	28.98	57.82	148.83
2	S2	30.00	10.80	148.83
3	N2	28.44	12.91	148.83
4	K1	15.04	12.22	74.42
5	O1	13.94	7.78	74.42
6	M4	57.97	1.10	297.67

3.2 Calibration for the storativity/transmissivity ratio

Knowing the tidal parameters as in Table 1, the series expansion (3) for the

q_k's are calculated from eq. (4) and (5), respectively, assuming an initial S/T ratio which is then refined during the calibration procedure. Moreover, since tidal friction in the open water along the shore can be neglected, the damping coefficient m_k in eq. (3) has been set to zero.

During the calibration of the S/T-ratio, the predicted heads are compared with the measured ones. However, before doing so, the raw data has to be filtered to remove all non-tidal fluctuations caused e.g. by precipitation and storm surges. This "detrending" is performed by means of standard 24- 25-hour moving- average filters (*Fig. 2*) (*Godin, 1972; Hsieh et al.,1987*).

Results of a few calibration runs are shown in *Fig.3*. For the *Galen well* one notices that the *S/T*-ratio has a stronger effect on the phase than on the amplitude (compare *Figs.3a* and *3b*). In accordance with eq. (3) the amplitude of the predicted head is more controlled by the inland-distance x from the coastline than by the *S/T*-ratio. Moreover, it can be seen that the match between the predicted and the measured head data is not equally good over the one-month observation period. For example, with a preselected storativity value of $S=0.002$, the values for the transmissivity in the two *S/T*-calibrations for the *Galen well* are T= 93 m^2/day in *Fig. 3a* and T=98 m^2/day in *Fig. 3b*, respectively. With the former value, the predicted head matches the measured data very well in late July (*Fig.3a*), but is approximately one and a half hour out of phase in early July. With the latter value, on the other hand, the situation is just the opposite, with a good match now in early July (*Fig. 3b*). Re-examining the original head data (*Fig. 2a*), it can be seen that in the beginning of July 1994 the piezometric head is almost 2m higher than in late July. Since for a confined aquifer the head h is directly correlated with the hydraulic pressure p through $p= \rho g h$ [M/LT^2] (ρ = density of water), one may conjecture that the *S/T*-ratio itself is not constant, but varies with the pressure. Theoretically, the storativity S is more likely to be sensitive to pressure than the transmissivity T, because S for a confined aquifer is calculated through the well-known formula $S = \rho g\, B(\alpha + n\beta)$, where α [LT^2/M] and β [LT^2/M] are the compressibilities of the aquifer matrix and the water, respectively, and n is the porosity *(Bear, 1972)*. Since it is conceivable that α decreases with higher pressure, a reduced value for S is consistent with the lower *S/T-ratio* needed to get the good match to the high measured hydraulic heads in early July.

Whereas the *Galen well,* because of its location, is affected by the open Atlantic Ocean tide, the water levels in the *Firehouse well*---which is located close to the inland estuary (*Fig. 1*)---react more to the tide there. An approximate six-hour phase difference exists between the tides at these two locations. Note the very good fit of both the amplitude and the phase of the predicted data with the filtered measured data for the *Firehouse well* (*Fig.4c*) which might be a consequence of the stronger observed signals at this well, but

shows clearly the superiority of the present 2D-calibrations over the 1D approach of earlier studies mentioned in the introduction.

3.3 Calculation of water particle trajectories

Once the *S/T*-ratio has been calibrated, Darcy-flow velocities of the water particles are calculated using eq. (7). It should be noted that large depression cones exist near the study site, as a consequence of heavy pumping that has occurred recently in the wake of construction of several new casinos in Atlantic City *(Smith and Sun, 1996)*. The groundwater flow along the coast is, therefore, slightly directed toward Atlantic City. *Fig. 4* shows stick plots of the predicted Darcy-flow velocities over a period of 3 days. The tidal effects can be clearly seen from the varying magnitudes and the changing directions of the velocity vectors. However, because of the superposition of regional- and tidally induced flow (eq. 6), the average total Darcy-flow velocity does not change in a coastal aquifer, despite a longer path traveled by water particles near the shore.

Particle trajectories calculated with eq. (8) are shown in *Fig. 5*for the *Galen well* calibration and in *Fig. 6* for the *Firehouse well* calibration. Water particles are moving back and forth as the hydraulic gradient changes every 12 and 24 hours. This zigzag movement of the groundwater front is stronger at a location closer to the coast (*Figs. 5a* and *6a*) than farther inland (*Figs. 5b,c* and *6b*) where the damping effect comes into play. This is also the reason for the overall stronger undulations of the water particles for the *Firehouse well* (*Fig. 6*) which is closer to the shore than the *Galen well* (*Fig. 1*). In any case, a unique 'flushing' effect is created in the coastal aquifer that would carry away and disperse dissolved solute (contaminant) particles in the groundwater more effectively than regional flow alone. This 'flushing' effect should be taken into consideration when the hydraulic removal of a contaminant along the coastal aquifer is modeled.

References

Bear, J., *Dynamics of fluids in porous media*, Elsevier, New York, NY, 1972.

Boon, J. D. and K.P. Kiley, *Harmonic analysis and tidal prediction by the method of least squares*, Special Report No.186, Virginia Institute of Marine Science, Glocester Point, Virginia, 1978.

Carr, P. A. and G.S. Van Der Kamp, Determining aquifer characteristics by the tidal method, *Water Resour. Res.*, 5, 1023-1031, 1969.

Dean, R.G. and R.A. Dalrymple, *Water wave mechanics for engineers and scientists*, Prentice Hall, Inc., Englewood Cliffs, NJ, 1984.

Godin, G., *The analysis of tides*. University of Toronto Press, Toronto, 1972.
Gregg, D. O., An analysis of ground water fluctuation caused by ocean tides in Glynn County, Georgia. *Ground Water*, .4, 211-232, 1966.
Hsieh, P.A., J.D. Bredehoeft and J.M. Farr, Determination of aquifer transmissivity from earth tide analysis, *Water Resour. Res.*,.23, 1824-1832, 1987.
Nielsen, P., Tidal dynamics of the water table in Beaches, *Water Resour. Res.*, 26,. 2127-2134, 1990.
Parker, B. B., *Tidal Hydrodynamics*, John Wiley & Sons, New York, NY, 1991.
Serfes, M. E., Determining the mean hydraulic gradient of ground water affected by tidal fluctuations, *Ground Water*, 29, 549-555, 1992.
Smith, J. and H. Sun, Potential problems of groundwater resources depletion and water quality deterioration in the state of New Jersey in 1997. *American Geophysical Union, Transactions (EOS)*, 77, 17, 1996.
Sun, H., A two-dimensional analytical solution of groundwater response to tidal loading in an estuary, *Water Resour. Res.*, 32, 1997.
USGS, Water Resources Data New Jersey, Water Year 1994, U.S. *Geological Survey Water Report NJ-94-2*, 1994.
Yim, C.S. and M.F..N. Mohsen, Simulation of tidal effects on contaminant transport in porous media, *Ground Water*, 30, 78-86, 1992.

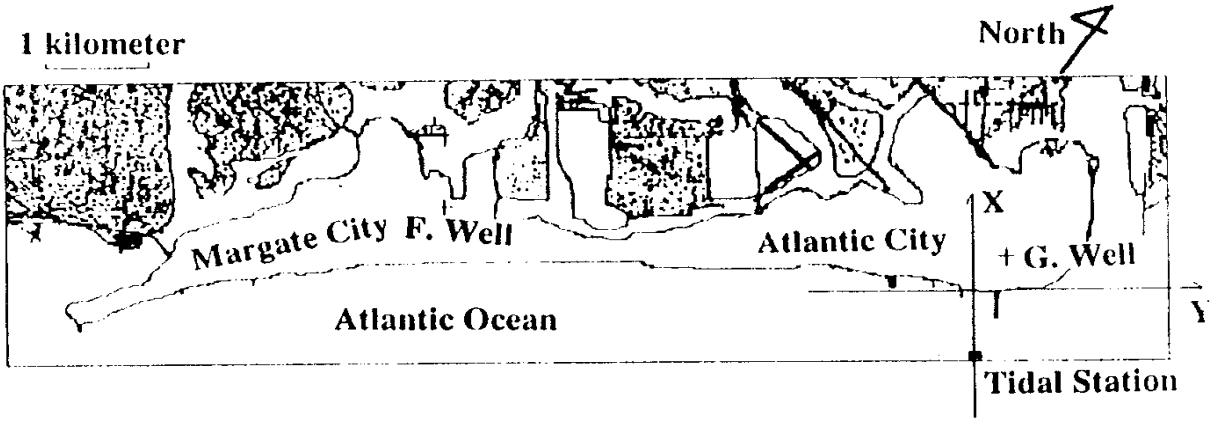

Fig. 1 Map of Atlantic City area with locations of the wells and the tidal station. G.Well = Galen well, F. Well = Firehouse well.

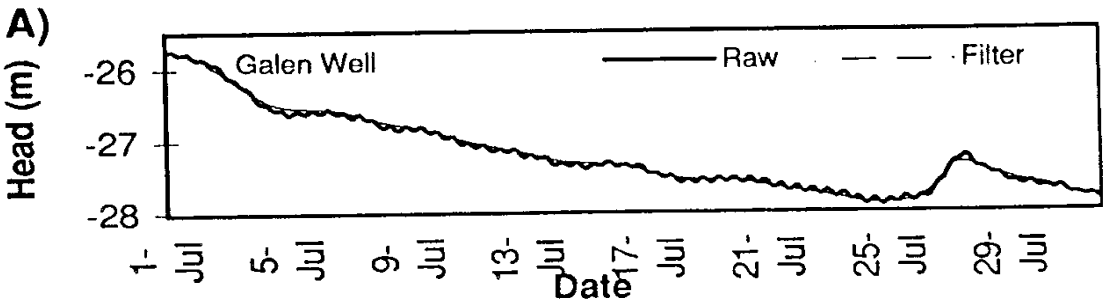

Fig. 2

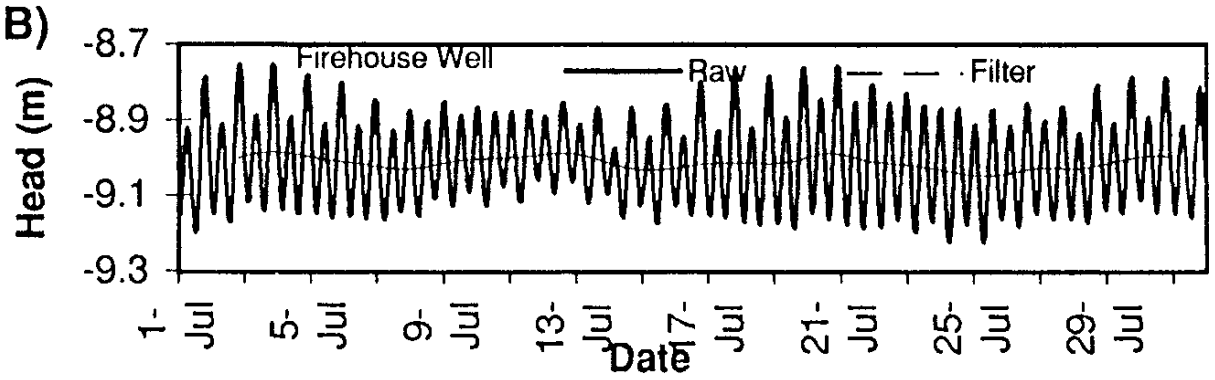

Fig. 2 Diagrams of the raw piezometric data (thick line) and of the filtered data (thin line). A) Galen well; B) Firehouse well.

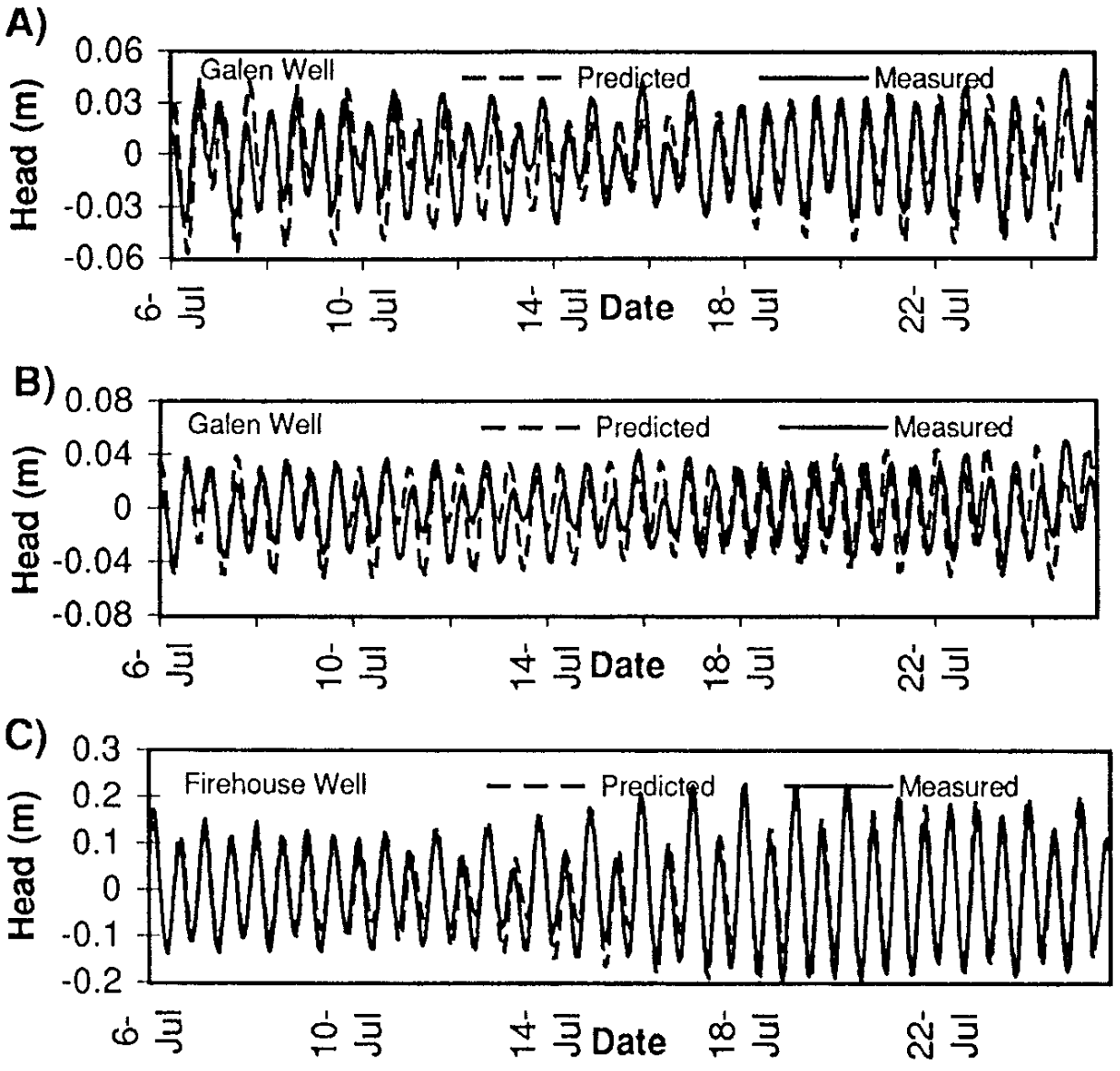

Fig. 3 Results of S/T-ratio calibration. With a constant S=0.002, T is varied. A) Galen well, S/T=2.15*10-5 day/m^2 (T=93m2/day); B) Galen well, S/T=2.04*10-5 day/m^2 (T=98m^2/day); C) Firehouse well, S/T=2.14*10-5 day/m^2 (T=93.5m^2/day).

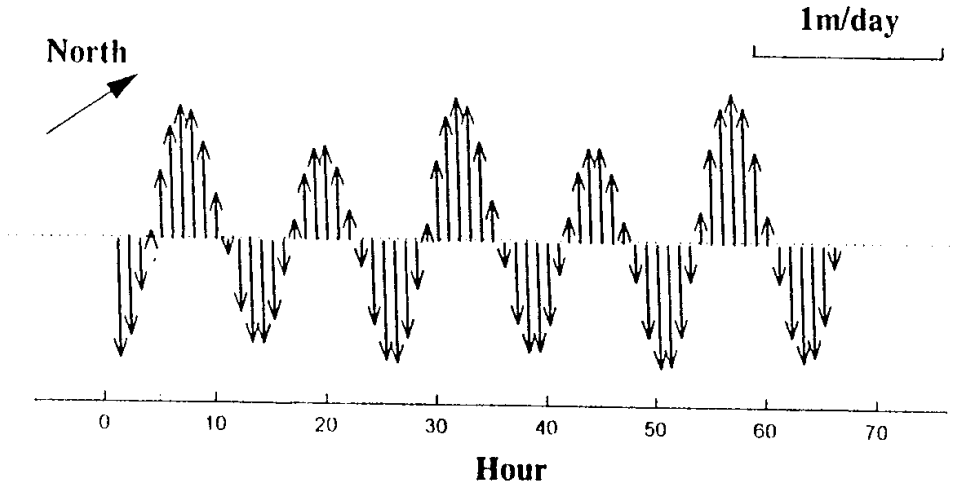

Fig. 4 Stick plots of the calculated hourly flow velocity from July 6 to July 8, 1994 with T=93 m^2/day at location x=5, y=5 meters near Firehouse well.

Fig. 5

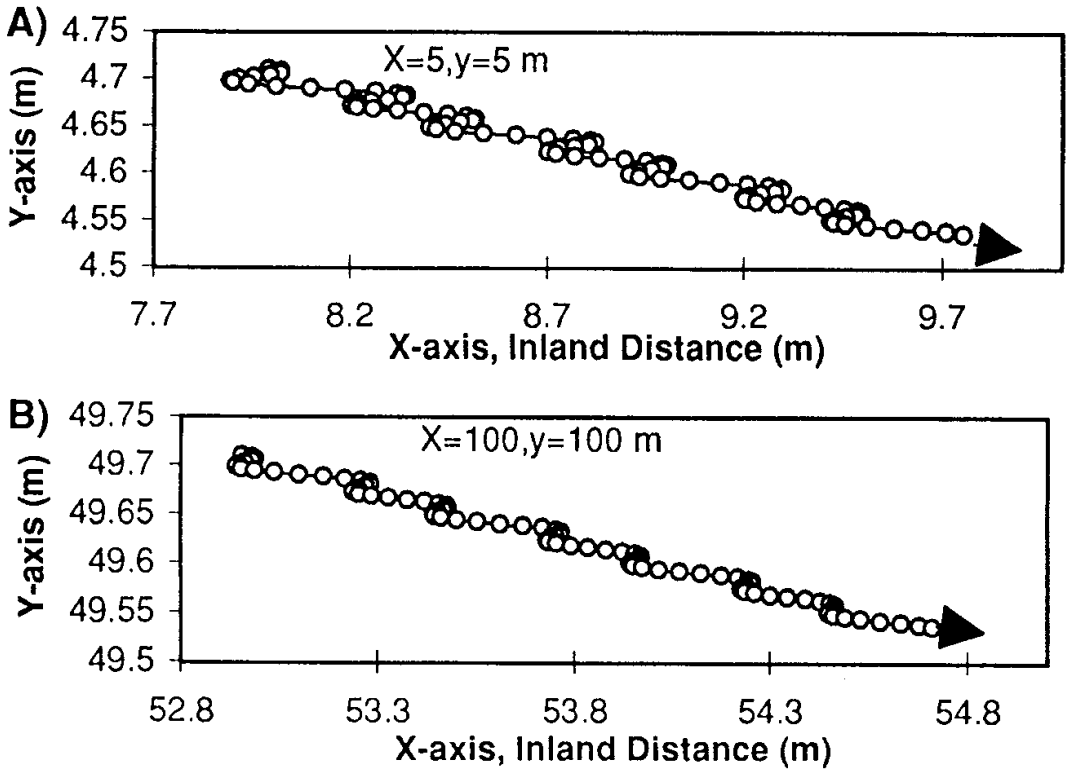

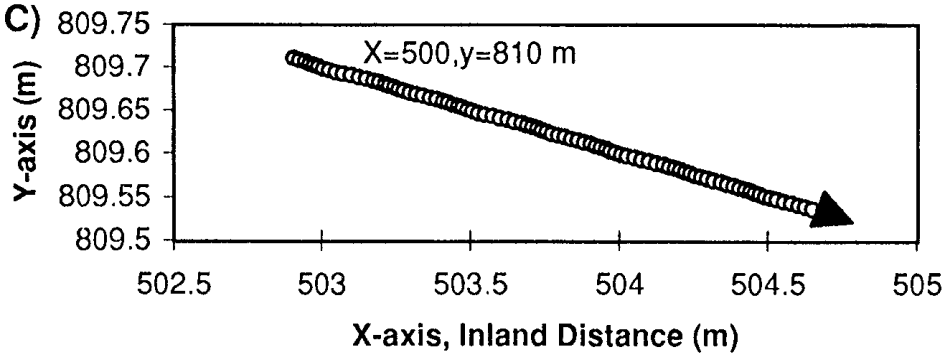

Fig. 5 Trajectory of water particle for the flow at Galen Well from July 6 to July 8, 1994. A) at location x=5, y=5 meters; B) at location x=100, y=100 meters; C) at location x=500, y=810 meters.

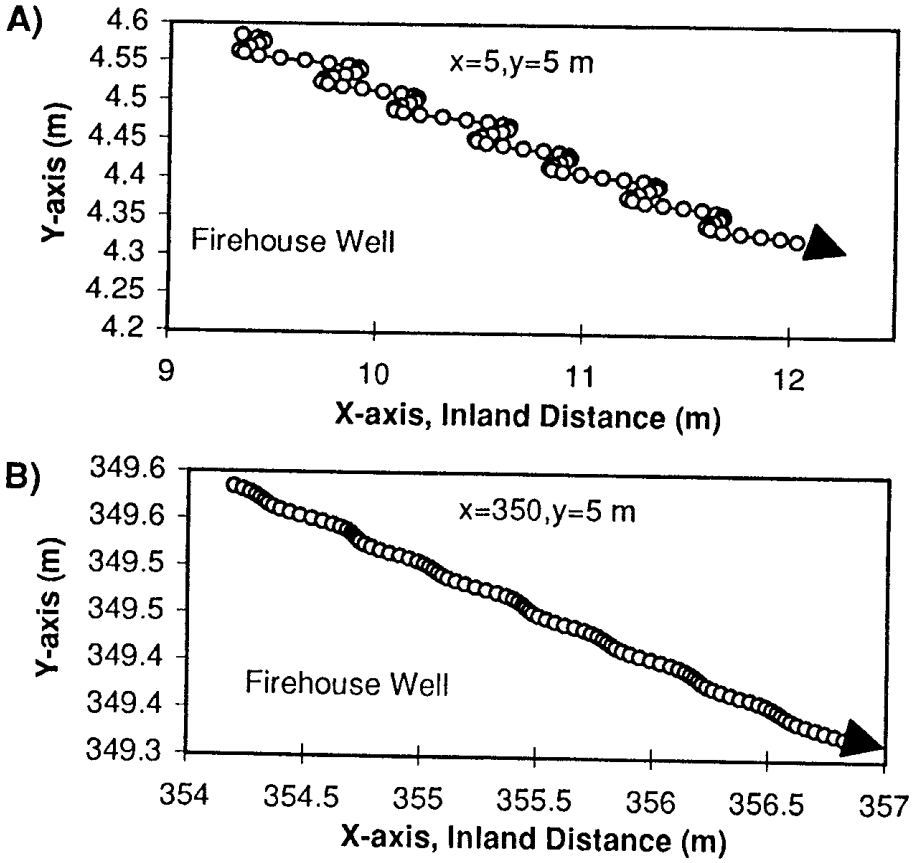

Fig. 6 Trajectory of water particle for the flow at Firehouse well from July 6 to July 8, 1994. A) at location x=5, y=5 meters; B) at location x=350, y=5 meters.